Reactions of thiyl radicals with phosphines or phosphites produce initially a phosphoranyl radical (eq 18, Z = R′ or OR′),

$$RS^{\bullet} + Z_3P \rightarrow (Z_3PSR)^{\bullet} \quad (18)$$

generally followed by C–S homolysis to give an organophosphorus sulfide and an organic radical (eq 19).[35-39] This latter step was

$$(Z_3PSR)^{\bullet} \rightarrow Z_3PS + R^{\bullet} \quad (19)$$

not observed for the current system, however, as it required sulfur abstraction from a bridge. Alternative modes of decomposition of the presumed dimer–phosphoranyl radical intermediate $[SMo_2SPZ_3]^{\bullet}$ were therefore found. For triethyl phosphite, C–O fission gave the observed ethanethiolate-bridged dimer and the proposed (*O,O′*-diethyl thiophosphato-*S*)-bridged dimer (eq 10). C–O homolysis is indeed known for thiyl–phosphite systems as an alternative to eq 19, but it is a relatively minor pathway.[39-41] For triphenylphosphine the overall reaction, eq 8, resembled previous nucleophilic reductions,[18] but the radical mechanism here was not clearly discernible. There may have been direct acetate involvement with the radical site to account for the observed products.

Other Systems. The chemistry herein described, while an obvious mimicry of diorganyl disulfide chemistry, knows a limited parallel in metal–sulfur systems. Photochemistry of such compounds has, of course, been investigated, but not so much in terms of S–S photohomolysis.[42] Photochemical reactions of metal complexes with diorganyl disulfides are known to give metal thiolates[43] or, for organocobaloximes, thioethers;[44] these therefore do not involve new S–S bonds in the products. An increasing variety of disulfide complexes are known,[45] but the majority of these involve bidentate disulfide, or the disulfide is one component of a multiply bridged oligomer. S–S photolability would be expected to be less demonstrable, albeit not impossible, in these types and more readily observable in systems wherein a single S–S linkage bridges two fragments capable of at least a transitory existence.

Several examples of photolabile metal S–S compounds are noted. S–S photohomolysis has been reported for dithionite bridges in $[(C_5H_5)Fe(CO)_2SO_2]_2$ and $[Mn(CO)_5SO_2]_2$.[46] Monomeric, radical intermediates were implicated. $[(H_2NC_2H_4NH_2)_2Co(OH_2)(S_2O_3)]^+$, containing a Co–S(S)–$SO_3$ unit, has demonstrated photosensitivity to fluorescent lighting, although S–S cleavage was not explicitly indicated.[47] $[(C_5H_5)Fe(CO)_2]_2S_3$, a trisulfide-bridged iron dimer, was also reported to be light sensitive in solution, but again the nature of the photolability was not indicated.[48] Photoisomerization has been observed for the $[(Me_5C_5)MoS_2]_2$ system and involves sulfide–disulfide interconversions.[49] One component of that process actually has a multiple bridge involving disulfide and sulfide sites, but presumably dimer dissociation does not occur and radical monomers are not involved.

Acknowledgment. This work was supported by Research Awards from the Graduate School and from the College of Arts and Sciences of the University of Louisville.

(37) Mackie, R. K. In *Organophosphorus Reagents in Organic Synthesis*; Cadogan, J. I. G., Ed.; Academic: London, 1979; p 351.
(38) Bentrude, W. G. In *Free Radicals*; Kochi, J. K., Ed.; Wiley-Interscience: New York, 1973; Vol. 2, p 595.
(39) Walling, C.; Rabinowitz, R. *J. Am. Chem. Soc.* **1959**, *81*, 1243.
(40) Walling, C.; Basedow, O. H.; Savas, E. S. *J. Am. Chem. Soc.* **1960**, *82*, 2181.
(41) Walling, C.; Pearson, M. S. *J. Am. Chem. Soc.* **1964**, *86*, 2262.
(42) Deutsch, E.; Root, M. J.; Nosco, D. L. *Adv. Inorg. Bioinorg. Mech.* **1982**, *1*, 269.
(43) See, for example: Jaitner, P. *J. Organomet. Chem.* **1981**, *210*, 353; **1982**, *231*, 225. Abrahamson, H. B.; Freeman, M. L. *Organometallics* **1983**, *2*, 679.
(44) Deniau, J.; Duong, K. N. V.; Gaudemer, A.; Bougeard, P.; Johnson, M. D. *J. Chem. Soc., Perkin Trans. 2* **1981**, 393.
(45) Müller, A.; Jaegermann, W.; Enemark, J. H. *Coord. Chem. Rev.* **1982**, *46*, 245.
(46) Poffenberger, C. A.; Tennent, N. H.; Wojcicki, A. *J. Organomet. Chem.* **1980**, *191*, 107.
(47) Mittleman, J. P.; Cooper, J. N.; Deutsch, E. A. *J. Chem. Soc., Chem. Commun.* **1980**, 733.
(48) El-Hinnawi, M. A.; Aruffo, A. A.; Santarsiero, B. D.; McAlister, D. R.; Schomaker, V. *Inorg. Chem.* **1983**, *22*, 1585.
(49) Bruce, A. E.; Tyler, D. R. *Inorg. Chem.* **1984**, *23*, 3433.

Contribution from the Kenan Laboratories of Chemistry, The University of North Carolina, Chapel Hill, North Carolina 27514

Synthesis and Electropolymerization of Distyrylbipyridine and Methyldistyrylbipyridine Complexes of Iron, Ruthenium, Osmium, Rhenium, and Cobalt

C. R. Leidner,† B. Patrick Sullivan,* R. A. Reed, B. A. White, M. T. Crimmins, Royce W. Murray,* and Thomas J. Meyer

Received June 25, 1986

Several dozen Fe, Ru, Os, Re, and Co complexes containing the ligands 4,4′-distyryl-2,2′-bipyridine (DSB) and 4,4′-bis(*p*-methylstyryl)-2,2′-bipyridine (MeDSB) have been prepared. The ligands undergo coupling reactions when the complexes are reduced electrochemically, resulting in the formation of smooth and adherent electroactive polymeric films on Pt electrodes. Evaluation of the relative rates of electropolymerization for selected metal complex monomers shows that the DSB and MeDSB ligands lead to slower electropolymerizations than do the related ligands vbpy (4-vinyl-4′-methyl-2,2′-bipyridine) and vpy (4-vinylpyridine) in analogous complexes. The stability of the DSB and MeDSB ligands was helpful in the synthesis of novel electropolymerizable monomers such as $[Os(DSB)_3]^{2+}$, $[Os(MeDSB)_3]^{2+}$, $[(DSB)_2M(CO)Cl]^+$ (M = Ru, Os), and $[(DSB)Re(CO)_3X]$. The last complex is a CO_2 reduction catalyst. Correlations between monomer composition and polymer characteristics were revealing, showing, for example, that poly-$[(MeDSB)_3M]^{2+}$ films exhibit faster electron transport and are more permeable than previously studied poly-$[Ru(vbpy)_3]^{2+}$ films.

The realization that electrocatalysis with chemically modified electrodes should be most effective with an electroactive polymer film catalyst possessing an accessible interior and fast electron transport has been one of several factors behind the development of electroactive polymer coatings for electrodes.[1,2] The most common types of coatings are polymers with covalently attached redox sites and ion-exchange polymers with electroactive counterions. Ion-exchange polymers[3-17] are attractive in that a given

* To whom correspondence should be addressed.
† Present address: Department of Chemistry, Purdue University, West LaFayette, IN.

(1) Andrieux, C. P.; Dumas-Bouchiat, J. M.; Saveant, J.-M. *J. Electroanal. Chem. Interfacial Electrochem.* **1981**, *123*, 171.
(2) Murray, R. W. *Philos. Trans. R. Soc. London, A* **1981**, *302*, 253.
(3) Oyama, N.; Anson, F. C. *J. Am. Chem. Soc.* **1979**, *101*, 739.

0020-1669/87/1326-0882$01.50/0

Table I. Monomeric Complexes Containing the Distyrylbipyridine and (Methylstyryl)bipyridine Ligands[a]

$[(DSB)_{3-n}Ru(bpy)_n](PF_6)_2$ (n = 0–2)	$[Fe(MeDSB)_3](PF_6)_2$
$[(MeDSB)_{3-n}Ru(bpy)_n](PF_6)_2$ (n = 0–2)	$[(DSB)_{3-n}Os(bpy)_n](PF_6)_2$ (n = 0–2)
$[(DSB)_2RuCl_2]\cdot 2H_2O$	$[(MeDSB)_{3-n}Os(bpy)_n](PF_6)_2$ (n = 0–2)
$[(MeDSB)_2RuCl_2]\cdot 2H_2O$	$[(DSB)_2OsCl_2]\cdot 2H_2O$
$[(DSB)_2Ru(CH_3CN)_2](PF_6)_2$	$[(MeDSB)_2OsCl_2]\cdot 2H_2O$
$[(MeDSB)_2Ru(CH_3CN)_2](PF_6)_2$	$[(DSB)_2Os(CO)Cl](PF_6)$
$[(DSB)_2Ru(pyrc)](PF_6)$	$[Co(DSB)_3](PF_6)_2$
$[(DSB)_2Ru(bpym)](PF_6)_2$	$[Co(MeDSB)_3](PF_6)_2$
$[(DSB)_2Ru(CO)Cl](PF_6)$	$[(DSB)Re(CO)_3Cl]$
$[Fe(DSB)_3](PF_6)_2$	

[a] Abbreviations: DSB = 4,4′-distyryl-2,2′-bipyridine; MeDSB = 4,4′-bis(*p*-methylstyryl)-2,2′-bipyridine; bpym = 2,2′-bipyrimidine; pyrc = 2-pyrazinecarboxylate.

polymer coating can accommodate a variety of catalyst redox counterions, and the redox counterions are often quite mobile[12-16] and give rapid electron transport. Unfortunately, the redox counterions tend to leach out of ion-exchange polymers, which lowers the electron transport rate and the catalyst activity.[17]

Polymer films with covalently fixed redox sites are more difficult to achieve synthetically but can yield significant electron mobilities and systematically variable chemical properties. Examples include poly(vinylferrocene) (PVFer),[18-23] polyviologens,[24-31] polymeric metalloporphyrins,[32,33] and metal-based polypyridyl complexes.[34-40] In earlier work it was shown that $[(bpy)_2Ru(vpy)_2]^{2+}$, where bpy = 2,2′-bipyridine and vpy = 4-vinylpyridine, could be reductively electropolymerized from several solvents, notably acetonitrile, to form thin (10–1000 m) electroactive films on Pt electrodes.[34] Subsequently, the electropolymerization procedure was used to prepare films from other vinyl-containing metal polypyridyl and analogous complexes,[34-37] including homopolymeric films and copolymeric films[35,41,42] and bilayers.[34,35,43-45] The resulting films have found application in studies of electron transport,[41,42] electron-transfer reactions,[46-49] film permeation,[42,48,50] sandwich cells,[51-53] electronic devices,[53] and photoelectrochemical phenomena.[54]

We report here the electropolymerization of complexes containing the ligands 4,4′-distyryl-2,2′-bipyridine (DSB) and 4,4′-bis(*p*-methylstyryl)-2,2′-bipyridine (MeDSB) and their Fe, Ru, Os, Re, and Co complexes (Table I). The DSB and MeDSB

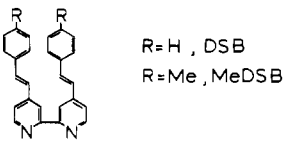

ligands themselves are thermally less reactive toward polymerization than the vpy (4-vinylpyridine) and vbpy (4-vinyl-4′-methyl-2,2′-bipyridine) ligands employed in our previous work. Consequently, DSB and MeDSB can be used to prepare electropolymerizable monomers that owing to the forcing reaction conditions required are not readily obtainable with vpy or vbpy. Examples are the complexes $[Os(DSB)_3]^{2+}$, $[Os(MeDSB)_3]^{2+}$, $[(DSB)_2M(CO)Cl]^+$ (M = Ru, Os), $[Ru(DSB)_2X_2]^{n+}$, and $[Ru(MeDSB)_2X_2]^{n+}$. As an illustration, the complexes $[(DSB)_2M(CO)Cl]^+$ (M = Ru, Os) are prepared by heating the corresponding $[(DSB)_2MCl_2]$ complexes in formic acid overnight at reflux. The thermal stability of the DSB and MeDSB ligands

(4) Oyama, N.; Anson, F. C. *J. Am. Chem. Soc.* **1979**, *101*, 3450.
(5) Facci, J. S.; Murray, R. W. *J. Electroanal. Chem. Interfacial Electrochem.* **1981**, *124*, 339.
(6) Facci, J. S.; Murray, R. W. *J. Phys. Chem.* **1981**, *85*, 2870.
(7) Kuo, K. N.; Murray, R. W. *J. Electroanal. Chem. Interfacial Electrochem.* **1982**, *131*, 37.
(8) Schneider, J. R.; Murray, R. W. *Anal. Chem.* **1982**, *54*, 1508.
(9) Rubinstein, I.; Bard, A. J. *Anal. Chem.* **1981**, *53*, 102.
(10) Bruce, J. A.; Wrighton, M. S. *J. Am. Chem. Soc.* **1982**, *104*, 7420.
(11) Buttry, D. A.; Anson, F. C. *J. Am. Chem. Soc.* **1982**, *104*, 4824.
(12) Mortimer, R. J.; Anson, F. C. *J. Electroanal. Chem. Interfacial Electrochem.* **1982**, *138*, 325.
(13) Anson, F. C.; Saveant, J.-M.; Shigehara, K. *J. Am. Chem. Soc.* **1983**, *105*, 1096.
(14) Buttry, D. A.; Anson, F. C. *J. Am. Chem. Soc.* **1983**, *105*, 685.
(15) Buttry, D. A.; Saveant, J.-M.; Anson, F. C. *J. Phys. Chem.* **1984**, *88*, 3086.
(16) White, H. S.; Leddy, J.; Bard, A. J. *J. Am. Chem. Soc.* **1982**, *104*, 4811.
(17) Buttry, D. A.; Anson, F. C. *J. Electroanal. Chem. Interfacial Electrochem.* **1981**, *130*, 333.
(18) Merz, A.; Bard, A. J. *J. Am. Chem. Soc.* **1978**, *100*, 3222.
(19) Flanagan, J. B.; Margel, J. S.; Bard, A. J.; Anson, F. C. *J. Am. Chem. Soc.* **1978**, *100*, 4248.
(20) Peerce, P. J.; Bard, A. J. *J. Electroanal. Chem. Interfacial Electrochem.* **1980**, *108*, 121.
(21) Daum, P.; Lenhard, J. R.; Rolison, D. R.; Murray, R. W. *J. Am. Chem. Soc.* **1980**, *102*, 4649.
(22) Daum, P.; Murray, R. W. *J. Electroanal. Chem. Interfacial Electrochem.* **1979**, *103*, 289.
(23) Rolison, D. R.; Umana, M.; Burgmayer, P.; Murray, R. W. *Inorg. Chem.* **1981**, *20*, 2996.
(24) Mortimer, R. J.; Anson, F. C. *J. Electroanal. Chem. Interfacial Electrochem.* **1982**, *139*, 325.
(25) Abruna, H. D.; Bard, A. J. *J. Am. Chem. Soc.* **1981**, *103*, 6898.
(26) Willman, K. W.; Murray, R. W. *J. Electroanal. Chem. Interfacial Electrochem.* **1982**, *133*, 211.
(27) Burgmayer, P.; Murray, R. W. *J. Electroanal. Chem. Interfacial Electrochem.* **1982**, *135*, 335.
(28) Bookbinder, D. G.; Lewis, N. S.; Bradley, M. G.; Bocarsly, A. B.; Wrighton, M. S. *J. Am. Chem. Soc.* **1979**, *101*, 7721.
(29) Dominey, R. N.; Lewis, T. J.; Wrighton, M. S. *J. Phys. Chem.* **1983**, *87*, 5345.
(30) Elliott, C. M.; Martin, W. S. *J. Electroanal. Chem. Interfacial Electrochem.* **1982**, *137*, 377.
(31) Oyama, N.; Yamaguchi, S. *J. Electroanal. Chem. Interfacial Electrochem.* **1982**, *139*, 215.
(32) Macor, K. A.; Spiro, T. G. *J. Am. Chem. Soc.* **1983**, *105*, 5601.
(33) White, B. A.; Murray, R. W. *J. Electroanal. Chem. Interfacial Electrochem.* **1985**, *189*, 345.
(34) Abruna, H. D.; Denisevich, P.; Umana, M.; Meyer, T. J.; Murray, R. W. *J. Am. Chem. Soc.* **1981**, *103*, 1.
(35) Denisevich, P.; Abruna, H. D.; Leidner, C. R.; Meyer, T. J.; Murray, R. W. *Inorg. Chem.* **1982**, *21*, 2153.
(36) Calvert, J. M.; Schmehl, R. H.; Sullivan, B. P.; Facci, J. S.; Meyer, T. J.; Murray, R. W. *Inorg. Chem.* **1983**, *22*, 2151.
(37) Ghosh, P. K.; Spiro, T. G. *J. Electrochem. Soc.* **1981**, *128*, 1281.
(38) Hass, O.; Vos, J. G. *J. Electroanal. Chem. Interfacial Electrochem.* **1980**, *113*, 139.
(39) Hass, O.; Kriens, M.; Vos, J. G. *J. Am. Chem. Soc.* **1981**, *103*, 1318.
(40) Calvert, J. M.; Meyer, T. J. *Inorg. Chem.* **1981**, *20*, 27.
(41) Facci, J. S.; Schmehl, R. H.; Murray, R. W. *J. Am. Chem. Soc.* **1982**, *104*, 4959.
(42) Schmehl, R. H.; Murray, R. W. *J. Electroanal. Chem. Interfacial Electrochem.* **1983**, *152*, 97.
(43) Denisevich, P.; Willman, K. W.; Murray, R. W. *J. Am. Chem. Soc.* **1981**, *103*, 4727.
(44) Pickup, P. G.; Leidner, C. R.; Denisevich, P.; Murray, R. W. *J. Electroanal. Chem. Interfacial Electrochem.* **1984**, *164*, 39.
(45) Leidner, C. R.; Denisevich, P.; Willman, K. W.; Murray, R. W. *J. Electroanal. Chem. Interfacial Electrochem.* **1984**, *164*, 64.
(46) Ikeda, T.; Leidner, C. R.; Murray, R. W. *J. Am. Chem. Soc.* **1981**, *103*, 7422.
(47) Leidner, C. R.; Murray, R. W. *J. Am. Chem. Soc.* **1984**, *106*, 1606.
(48) Leidner, C. R.; Schmehl, R. H.; Pickup, P. G.; Murray, R. W. *Symposium on the Chemistry and Electrochemistry of Electrocatalysis*, San Francisco, CA, May 1983; McIntyre, J. D. E., Weaver, M., Yeager, E., Eds.; Electrochemical Society: Pennington, NJ, 1985.
(49) Ikeda, T.; Leidner, C. R.; Murray, R. W. *J. Electroanal. Chem. Interfacial Electrochem.* **1982**, *138*, 343.
(50) Ikeda, T.; Schmehl, R. H.; Denisevich, P.; Willman, K. W.; Murray, R. W. *J. Am. Chem. Soc.* **1982**, *104*, 2683.
(51) Pickup, P. G.; Murray, R. W. *J. Am. Chem. Soc.* **1983**, *105*, 4510.
(52) Pickup, P. G.; Kutner, W.; Leidner, C. R.; Murray, R. W. *J. Am. Chem. Soc.* **1984**, *106*, 1991.
(53) Pickup, P. G.; Murray, R. W. *J. Electrochem. Soc.* **1984**, *131*, 833.
(54) Margerum, L. D.; Murray, R. W.; Meyer, T. J. *J. Electroanal. Chem. Interfacial Electrochem.* **1983**, *149*, 2152.

is also reflected in slower rates of electrochemical polymerization than for analogous complexes containing vpy or vbpy.

Experimental Section

Chemicals. Acetonitrile (Burdick and Jackson) was stored over 3A molecular sieves. Tetraethylammonium perchlorate, Et_4NClO_4 (Eastman), tetrabutylammonium hexafluorophosphate, Bu_4NPF_6 (Eastman), and $LiClO_4$ (G. F. Smith) were recrystallized from water and stored in vacuo at 50 °C. Ferrocene was purified by sublimation. All other solvents and chemicals were reagent grade or better and were used as received.

Electrochemical Experiments. Electrochemical experiments were performed with standard three-electrode cells and instrumentation. Electropolymerizations were performed by placing a Teflon-shrouded Pt-disk electrode in a well-degassed solution of the monomer complex in 0.1 M Et_4NClO_4/CH_3CN and scanning the Pt electrode potential repetitively over a 1-V range that encompassed the formal potentials of the redox states responsible for electropolymerization. For example, with $[Ru(MeDSB)_3]^{2+}$ ($E^{\circ\prime}_{red}$ = −1.29, −1.42, and −1.64 V vs. SSCE) the potential was scanned repetitively between −0.74 and −1.74 V vs. SSCE at 100 mV/s. The polymer-coated electrode was washed with acetone and stored in air. Details of the film-permeation and electron-transport measurements are as described in our previous publications.[41,42,48,50]

Synthesis of 4,4′-Bis(*p*-methylstyryl)-2,2′-bipyridine (MeDSB) and 4,4′-Distyryl-2,2′-bipyridine (DSB). A mixture of 50.0 g (0.272 mol) of 4,4′-dimethyl-2,2′-bipyridine, 26.7 g (0.272 mol) of potassium acetate, 83 mL (86.7 g, 0.816 mol) of 4-methylbenzaldehyde, and a catalytic amount of iodine in 77 mL (83.1 g, 0.815 mol) of acetic anhydride was heated at reflux for 48 h. When the mixture was cooled to room temperature, the bis(methylstyryl)bipyridine precipitated and after filtration was recrystallized from $CH_3OCH_2CH_2OH$ to provide the pure 4,4′-(*p*-methylstyryl)-2,2′-bipyridine, yield 50.1 g (51%). Preparation of DSB was similar except that benzaldehyde was employed.

Synthesis of Metal Complexes. All reactions were performed under N_2 with magnetic stirring, unless otherwise noted. Preparations are described in detail for MeDSB as the entering ligand but apply essentially identically to the DSB ligand unless otherwise noted.

$[(MeDSB)_2RuCl_2]\cdot 2H_2O$ (or $[(DSB)_2RuCl_2]\cdot 2H_2O$). A 1.00-g (2.57-mmol) sample of MeDSB, 336 mg (1.337 mmol) of $RuCl_3\cdot 3H_2O$, and 250 mg of LiCl were heated at reflux in 40 mL of $CH_3OCH_2CH_2OH$ for 8 h. The solution was cooled to room temperature and placed in an ice bath overnight and the dark solution then filtered, yielding a dark purple solid and an orange-brown filtrate. The solid was washed with cold $CH_3OCH_2CH_2OH$ until the washings became faint purple (ca. 25 mL) and then with 70 mL of H_2O and 100 mL of diethyl ether and dried by suction; isolated yield 628 mg ($[(MeDSB)_2RuCl_2]\cdot 2H_2O$, 50%; $[(DSB)_2RuCl_2]\cdot 2H_2O$, 81%).

$[Ru(MeDSB)_3](PF_6)_2$ (or $[Ru(DSB)_3](PF_6)_2$). A 40-mg (0.153-mol) amount of $RuCl_3\cdot 3H_2O$ and 261 mg (0.723 mmol) of MeDSB were heated at reflux in 20 mL of DMF for 9.5 h. The solution was cooled to room temperature and filtered to remove the excess MeDSB. A 75-mL portion of H_2O and 20 mL of acetone were added to the solution. Addition of excess NH_4PF_6/H_2O led to precipitation of a red-orange solid. The solid was collected by suction filtration, washed with H_2O and diethyl ether, and purified by column chromatography (Al_2O_3, 2:1 toluene/CH_3CN). The red-orange band was collected and the solvent removed by rotary evaporation. The solid was reprecipitated with CH_3CN and ether and collected by suction filtration; isolated yield 150 mg ($[(MeDSB)_3Ru](PF_6)_2$, 64%; $[(DSB)_3Ru](PF_6)_2$, 85%).

$[(MeDSB)_2Ru(bpy)](PF_6)_2$. A 100-mg (0.102-mmol) amount of $[(MeDSB)_2RuCl_2]\cdot 2H_2O$ and 107 mg (0.683 mmol) of 2,2′-bipyridine were heated at reflux in 15 mL of DMF for 6 h. The solution was cooled to room temperature, and 40 mL of H_2O was added dropwise to the solution. Excess NH_4PF_6/H_2O was added to the stirring solution, yielding a flocculent red-orange solid. The sample was purified by column chromatography (2:1 toluene/CH_3CN) and reprecipitated from CH_3CN and diethyl ether; isolated yield 102 mg ($[(MeDSB)_2Ru(bpy)](PF_6)_2$, 76%).

$[(DSB)_2Ru(bpy)](PF_6)_2$. A 150-mg (0.161-mmol) amount of $[(DSB)_2RuCl_2]\cdot 2H_2O$ and 130 mg (0.083 mmol) of 2,2′-bipyridine were heated at reflux in 30 mL of 1:1 $H_2O/CH_3OCH_2CH_2OH$ for 4 h. Excess NH_4PF_6/CH_3OCH_2OH was added to the cooled reaction mixture, followed by slow addition of 10 mL of H_2O. The orange solid was collected, reprecipitated, and chromatographed on alumina with 3:2 toluene/CH_3CN; isolated yield 68 mg ($[(DSB)_2Ru(bpy)](PF_6)_2$, 33%).

$[(MeDSB)Ru(bpy)_2](PF_6)_2$. A 103-mg (0.199-mmol) amount of $[(bpy)_2RuCl_2]\cdot 2H_2O$[57] and 351 mg (0.904 mmol) of MeDSB were heated at reflux in 25 mL of 1:1 $EtOH/H_2O$ for 3 h. The solution was cooled to room temperature and then filtered to remove the excess MeDSB. The EtOH was removed by rotary evaporation, and excess NH_4PF_6/H_2O was added to the solution. The orange solid was collected by suction filtration and purified as above; isolated yield 168 mg ($[(MeDSB)Ru(bpy)_2](PF_6)_2$, 77%).

$[(DSB)Ru(bpy)_2](PF_6)_2$. A 211-mg (0.338-mmol) amount of $[(bpy)_2RuCl_2]\cdot 2H_2O$ and 291 mg (0.806 mmol) of DSB were heated at reflux in 30 mL of DMF for 4 h. The orange-brown solution was cooled to room temperature and worked up as for the analogous MeDSB complex; isolated yield 272 mg (66%).

$[(MeDSB)_2Ru(CH_3CN)_2](PF_6)_2$ (or $[(DSB)_2Ru(CH_3CN)_2](PF_6)_2$). A 152-mg (0.155-mmol) amount of $[(MeDSB)_2RuCl_2]\cdot 2H_2O$ was heated at reflux in 20 mL of 1:1:1 $H_2O/EtOH/CH_3CN$ for 10 h. The orange solution was filtered to remove the small amount of unreacted starting material. Excess NH_4PF_6/H_2O was added to the solution; the oily, orange solid was collected by suction filtration, washed with H_2O and diethyl ether, and purified by column chromatography (2:1 toluene/CH_3CN); isolated yield 165 mg ($[(MeDSB)_2Ru(CH_3CN)_2](PF_6)_2$, 85%; $[(DSB)_2Ru(CH_3CN)_2](PF_6)_2$, 85%).

$[Fe(DSB)_3](PF_6)_2$ (or $[Fe(MeDSB)_3](PF_6)_2$). A 57-mg (0.145-mmol) amount of $[Fe(NH_4)_2(SO_4)_2]\cdot 6H_2O$ and 211 mg (0.560 mmol) of DSB were heated at reflux in 50 mL of $CH_3OCH_2CH_2OH$ for 4.5 h. The reaction mixture was filtered to remove unreacted starting materials. Excess $NH_4PF_6/CH_3OCH_2CH_2OH$ was added to the solution. The purple solid was collected, unprecipitated, and purified by column chromatography (1:1 toluene/CH_3CN); isolated yield 97 mg ($[Fe(DSB)_3](PF_6)_2$, 47%; $[Fe(MeDSB)_3](PF_6)_2$, 47%).

$[(DSB)_2OsCl_2]\cdot 2H_2O$ (or $[(MeDSB)_2OsCl_2]\cdot 2H_2O$). A 202-mg (0.460-mmol) amount of $(NH_4)_2OsCl_6$ and 339 mg (0.941 mmol) of DSB were heated at reflux in 50 mL of $CH_3OCH_2CH_2OH$ for 2.5 h. The reaction mixture was cooled to room temperature and filtered. A 200-mg portion of $Na_2S_2O_4$ in 25 mL of H_2O was added to the brown filtrate; the resultant blue-black microcrystalline solid was collected by suction filtration and washed with cold $CH_3OCH_2CH_2OH$, H_2O, and diethyl ether. The crude product was suspended in 25 mL of warm (degassed) $CH_3OCH_2CH_2OH$ containing 80 mg of $Na_2S_2O_4$. After 10 min of stirring, the solution was cooled to room temperature under N_2 and the blue-black solid was collected and washed with H_2O and diethyl ether; isolated yield 292 mg ($[(DSB)_2OsCl_2]\cdot 2H_2O$, 62%). Yields ranged from 52 to 73% for other preparations.

$[Os(DSB)_3](PF_6)_2$. A 100-mg (0.229-mmol) amount of $(NH_4)_2OsCl_6$ and 416 mg (1.15 mmol) of DSB were heated at reflux in 30 mL of $CH_3OCH_2CH_2OCH_2CH_2OH$ for 3 h; the reaction mixture was cooled to room temperature and filtered. Excess $NH_4PF_6/CH_3OCH_2CH_2OCH_2CH_2OH$ was added to the brown filtrate; 30 mL of H_2O was added dropwise to the stirring solution. The precipitate was collected, washed with H_2O and diethyl ether, and reprecipitated with CH_3CN and ether. The crude brown sample was purified by column chromatography (1:1 toluene/CH_3CN); isolated yield 282 mg ($[(DSB)_3Os](PF_6)_2$, 79%).

$[Os(MeDSB)_3](PF_6)_2$. A 500-mg (1.14-mmol) amount of $(NH_4)_2OsCl_6$ and 4.450 g (11.4 mmol) of MeDSB were heated at reflux in 70 mL of $CH_3OCH_2CH_2OCH_2CH_2OH$ for 3.5 h. The reaction mixture was cooled to room temperature and added to 300 mL of H_2O. The solid was collected and purified (1:4 MeOH/CH_3CN); isolated yield 1.91 g ($[Os(MeDSB)_3](PF_6)_2$, 100%).

$[(DSB)_2Os(bpy)](PF_6)_2$. A 101-mg (0.100-mmol) amount of $[(DSB)_2OsCl_2]\cdot 2H_2O$ and 106 mg (0.68 mmol) of 2,2′-bipyridine were heated at reflux in $CH_3OCH_2CH_2OCH_2CH_2OH$ for 3 h. The solution was cooled, filtered, and worked up as for $[Os(DSB)_3](PF_6)_2$; isolated yield 87 mg ($[(DSB)_2Os(bpy)](PF_6)_2$, 65%).

$[(MeDSB)_2Os(bpy)](PF_6)_2$. A 100-mg (0.096-mmol) amount of $[(MeDSB)_2OsCl_2]\cdot 2H_2O$ and 170 mg (1.09 mmol) of 2,2′-bipyridine were heated at reflux in $CH_3OCH_2CH_2OCH_2OH$ for 3 h and worked up as for the DSB analogue; isolated yield 122 mg ($[(MeDSB)_2Os(bpy)](PF_6)_2$, 90%).

$[(DSB)Os(bpy)_2](PF_6)_2$ (or $[(MeDSB)Os(bpy)_2]$). A 233-mg (0.38-mmol) amount of $[Os(bpy)_2Cl_2]\cdot 2H_2O$[57] and 539 mg (1.49 mmol) amount of DSB were heated at reflux in 20 mL of ethylene glycol for 1 h. The green solid was collected and purified (2:1 toluene/CH_3CN); isolated yield 287 mg ($[(DSB)Os(bpy)_2](PF_6)_2$, 65%; $[(MeDSB)Os(bpy)_2](PF_6)_2$, 37%).

$[(DSB)_2Os(CO)Cl](PF_6)$. An 83-mg (0.081-mmol) amount of $[(DSB)_2OsCl_2]\cdot 2H_2O$ was heated at reflux in 90% formic acid for 10.5 h. The solution was cooled and taken to dryness by rotary evaporation. The red-orange solid was dissolved in 35 mL of 1:1 acetone/H_2O, and excess NH_4PF_6/H_2O was added dropwise to the stirring solution. The red solid was collected, washed with H_2O and diethyl ether, and purified by column chromatography (1:1 toluene/CH_3CN); isolated yield 60 mg ($[(DSB)_2Os(CO)Cl](PF_6)$, 66%).

$[(DSB)_2Ru(CO)Cl](PF_6)$. A 137-mg (0.147-mmol) amount of $[(DSB)_2RuCl_2]\cdot 2H_2O$ was heated at reflux in 90% formic acid and worked

Table II. Elemental Analysis Data[a]

compd	calcd				obsd			
	% C	% H	% N	% Cl	% C	% H	% N	% Cl
DSB	86.67	5.55	7.78		86.19	5.68	7.95	
MeDSB	86.56	6.23	7.21		85.13	6.49	8.01	
$[Ru(DSB)_3](PF_6)_2$	63.61	4.11	5.70		62.05	4.23	6.07	
$[Ru(MeDSB)_3](PF_6)_2$	64.81	4.67	5.40		60.31	4.52	6.02	
$[(DSB)_2Ru(CO)Cl](PF_6)$	61.77	3.92	5.43	3.44	60.18	4.04	5.41	3.47
$[(DSB)_3Os](PF_6)_2$	59.98	3.88	5.38		57.89	3.97	5.72	
$[(DSB)_2Os(CO)Cl](PF_6)$	56.85	3.61	5.00	3.17	54.85	3.73	5.16	3.76
$[(DSB)Re(CO)_3Cl]$	52.29	3.02	4.20	5.32	52.50	2.48	4.30	5.62

[a] NMR studies indicate that the ligands DSB and MeDSB contain a small fraction (<10%) of 4-styryl-4′-methyl-2,2′-bipyridine, which causes the analyses to have slightly higher nitrogen and hydrogen values and slightly lower carbon values than those calculated for theoretical stoichiometries. This "impurity" was equally present in all complexes and is assumed to have little consequence on the results presented in the text.

up as for the Os analogue; isolated yield 124 mg (82%).

$[(DSB)_2Ru(pyrc)](PF_6)$. A 199-mg (0.214-mmol) amount of $[(DSB)_2RuCl_2]\cdot 2H_2O$ and 54 mg (0.37 mmol) of pyrc (Aldrich) were suspended in 30 mL of 1:1 $H_2O/CH_3OCH_2CH_2OH$. A 1-mL portion of 2,6-dimethylpyridine was added, and the solution was heated at reflux overnight. The red solid was collected as the PF_6^- salt and purified (1:1 toluene/CH_3CN); isolated yield 168 mg (72%).

$[(DSB)Re(CO)_3Cl]$. A 150-mg (0.415-mmol) amount of $Re(CO)_5Cl$ and 165 mg (0.458 mmol) of DSB were heated at reflux in 50 mL of 1,2-dichloroethane for 8–10 h. The solution was cooled to room temperature and stirred for an additional 1.5 h, during which time an orange solid precipitates. The solid was collected via filtration, washed with three 10-mL portions of diethyl ether, and air-dried; isolated yield 243 mg (88.6%).

Results and Discussion

Synthesis and Purification. The two ligands 4,4′-distyryl-2,2′-bipyridine (DSB) and 4,4′-bis(*p*-methylstyryl)-2,2′-bipyridine (MeDSB) were prepared by the I_2-catalyzed condensation of 4,4′-dimethyl-2,2′-bipyridine with benzaldehyde and 4-methylbenzaldehyde, respectively. Recrystallization from 2-methoxyethanol yields a white solid that is sparingly soluble in acetone, 2-methoxyethanol, and 2-(2-methoxyethoxy)ethanol ($CH_3OCH_2CH_2OCH_2CH_2OH$). Due to the limited solubilities of these ligands, NMR characterization of the salt $[Os(MeDSB)_3](PF_6)_2$ was carried out in Me_2SO-d_6. A series of multiplets was observed in the expected aromatic region (δ = 7–9), and an upfield singlet at δ = 2.7 was observed for the methyl groups. The complexity of the aromatic region prohibits an accurate assessment of purity using NMR. The elemental analyses of the two ligands are given in Table II.

The syntheses of the DSB and MeDSB complexes were performed with slight modifications to procedures used previously for the analogous bpy complexes.[55-57] The primary difference between DSB and MeDSB complexes and bpy complexes is that the DSB and MeDSB ligands and the resultant metal complexes are less soluble. We found that 2-methoxyethanol and 2-(2-methoxyethoxy)ethanol dissolve the ligands well enough and have high enough boiling points (124 and 194 °C, respectively) to be good reaction solvents. DMF was employed as a solvent in some earlier syntheses, but the decomposition of DMF presumably leads to $[(L)_2Ru(CO)X]^{n+}$ impurities, which are difficult to completely remove with a single chromatographic run. Ruthenium, cobalt, and iron complexes were readily prepared in 2-methoxyethanol. Complexes of the type $[(L)_2OsCl_2]$ were also prepared in 2-methoxyethanol, but preparation of complexes of the type $[Os(L)_3]^{2+}$ required the higher boiling solvent 2-(2-methoxyethoxy)ethanol. The workup of the DSB and MeDSB complexes also reflects their more limited solubilities; their chloride salts are not water-soluble, so the metathesis procedure leading to PF_6^- salts had to be modified (see Experimental Section).

Purification of the DSB and MeDSB complexes by column chromatography is similar to that employed for the bpy analogues;[57] 1:1 toluene/CH_3CN on alumina is adequate for routine separations. The new complexes, however, often exhibit pronounced tailing on alumina, so that chromatographic bands with similar retention volumes often overlap. A second chromatographic run was consequently necessary for certain of the complexes, such as $[(L)_2Ru(CH_3CN)_2]^{2+}$, in which $[(L)_2Ru(CH_3CN)Cl]^+$ is present as an impurity. Despite the tailing, the purification is not difficult compared to that for other systems. The elemental analyses of selected complexes, given in Table II, tend to be somewhat lower in carbon and higher in nitrogen than ideal. Solutions of the complexes have the colors expected from their bpy analogues and exhibit very clean electrochemistry.

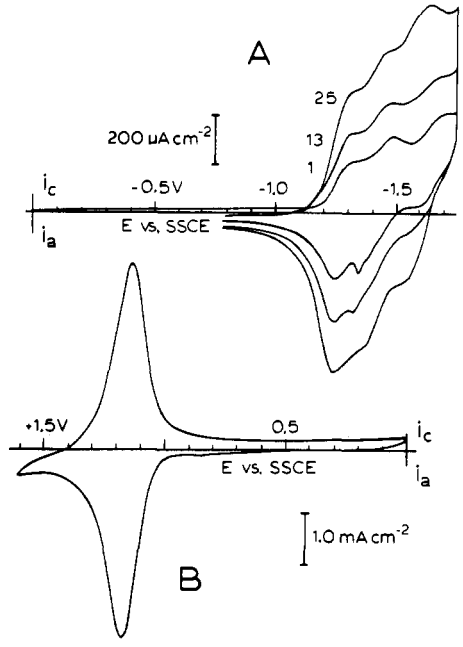

Figure 1. Cyclic voltammetry of (A) 0.67 mM $[(MeDSB)_3Ru]^{2+}$ in 0.1 M Et_4NClO_4/CH_3CN at 100 mV/s (potential scans 1, 13, and 25 from −0.74 to −1.74 V vs. SSCE shown) and (B) the Pt/poly-$[Ru(MeDSB)_3]^{2+}$ electrode prepared in Figure 1A in monomer-free 0.1 M Et_4NClO_4/CH_3CN at 100 mVs.

Electrochemistry and Electropolymerization. Ru Complexes. The various complexes of the type $[Ru(MeDSB)_x]^{2+}$ and $[Ru(DSB)_x]^{2+}$ (Table I) (as do their Os, Fe, and Co analogues) exhibit the anticipated redox properties as shown by cyclic voltammetry in 0.1 M Et_4NClO_4/CH_3CN. Reversible metal-centered Ru(III/II) oxidation waves are observed at positive potentials and a series of ligand-localized reduction waves at negative potentials. The reduction processes initiate the electropolymerization as is illustrated by the cyclic voltammograms of a 0.67 mM $[Ru(MeDSB)_3]^{2+}$ solution in CH_3CN shown in Figure 1A. The compound exhibits a succession of three reduction steps for the three MeDSB ligands, at −1.29, −1.42, and −1.64 V vs. SSCE. As the electrode potential is scanned through these waves between −0.74 and −1.74 V, there is a steady increase in the currents for the ligand-localized reductions (Figure 1A) and after 25 scans

(55) Powers, M. J.; Callahan, R. W.; Salmon, D. J.; Meyer, T. J. *Inorg. Chem.* **1976**, *15*, 894.
(56) Kober, E. M. Ph.D. Dissertation, The University of North Carolina, 1982.
(57) Sullivan, B. P.; Salmon, D. J.; Meyer, T. J. *Inorg. Chem.* **1978**, *17*, 3334.

Table III. M(III/II) Formal Potentials for Distyryl and Bis(methylstyryl) Ru and Os Complex Monomers and Their Electropolymerized Films

compd	$E^{\circ\prime}_{soln}$,[a] V vs. SSCE	$E^{\circ\prime}_{surf}$,[a] V vs. SSCE	Γ^*[b]
$[Ru(DSB)_3]^{2+/3+}$	1.10_5	1.16	1.0
$[(DSB)_2Ru(bpy)]^{2+/3+}$	1.14_5	1.18_5	0.33
$[(DSB)Ru(bpy)_2]^{2+/3+}$	1.20	1.22	0.032
$[Ru(MeDSB)_3]^{2+/3+}$	1.09	1.15	1.0
$[(MeDSB)_2Ru(bpy)]^{2+/3+}$	1.14	1.19	0.16
$[(MeDSB)Ru(bpy)_2]^{2+/3+}$	1.20_5	1.24	0.010
$[(DSB)_2Ru(CH_3CN)_2]^{2+/3+}$	1.28	1.36	0.23
$[(MeDSB)_2Ru(CH_3CN)_2]^{2+/3+}$	1.27	1.37	0.027
$[(DSB)_2Ru(pyrc)]^{+/2+}$	0.86	0.91	<0.001[c]
$[(DSB)_2Ru(bpym)]^{2+/3+}$	1.26_5	1.35	0.28
$[(DSB)_2Ru(CO)Cl]^{+/2+}$	1.41_5		
$[Os(DSB)_3]^{2+/3+}$	0.68_5	0.73	0.22
$[(DSB)_2Os(bpy)]^{2+/3+}$	0.72_5	0.75	0.03
$[(DSB)Os(bpy)_2]^{2+/3+}$	0.76	0.78_5	0.007
$[Os(MeDSB)_3]^{2+/3+}$	0.66	0.70	0.15
$[(MeDSB)_2Os(bpy)]^{2+/3+}$	0.72	0.75	0.07
$[(MeDSB)Os(bpy)_2]^{2+/3+}$	0.78	0.81	0.028
$[(DSB)_2Os(CO)Cl]^{+/2+}$	1.06	1.10	
$[(DSB)_2OsCl_2]^{0/+}$	−0.08		
$[(DSB)_2OsCl_2]^{+/2+}$	1.23		
$[(MeDSB)_2OsCl_2]^{0/+}$	−0.11		
$[(MeDSB)_2OsCl_2]^{+/2+}$	1.22		

[a] In 0.1 M Et_4NClO_4/CH_3CN. [b] Rate of electropolymerization measured by peak current growth (e.g., Figure 2); relative $\Gamma^* = 1.0$ for $[(MeDSB)_3Ru]^{2+}$. [c] Difficult to measure due to limited solubility of the complex in 0.1 M Et_4NClO_4/CH_3CN.

the Pt electrode is coated with a smooth orange film of poly-$[Ru(MeDSB)_3]^{2+}$. The increase in current is attributable to the combined electroactivity of the polymeric film and that of fresh, inward-diffusing monomer; both contribute to the continued, nonpassivating film growth. The shapes of the voltammetric waves shown in Figure 1A are typical of DSB and MeDSB complexes reported here in that the anodic return waves show irregular shapes akin to desorptive spikes. Despite the irregular shapes of the waves for the MeDSB complexes, the compounds are well-behaved with respect to electropolymerization.

In monomer-free 0.1 M Et_4NClO_4/CH_3CN, the coated Pt/poly-$[Ru(MeDSB)_3]^{2+}$ electrode gives cyclic voltammetry (Figure 1B) typical of electrodes coated with metal polypyridine films.[34-37] A stable, reversible Ru(III/II) wave is observed with small separation between oxidative and reductive waves ($\Delta E_p < 20$ mV) and little or no diffusional tailing. The formal potential for the Ru(III/II) couple in the polymer calculated as the average of $E_{p,a}$ and $E_{p,c}$ is $E^{\circ\prime}_{surf} = 1.15$ V vs. SSCE. The potential is nearly the same as that observed for a solution containing the monomer at a naked Pt electrode, $E^{\circ\prime}_{soln} = 1.09$ V vs. SSCE. Integration of the charge under either the cathodic or anodic wave gives a coverage of electroactive Ru(III/II) sites of $\Gamma_T = 6.3 \times 10^{-9}$ mol/cm^2, corresponding to ca. 60 monolayers of metal complex. The anodic and cathodic peak currents are equal and proportional to the scan rate ($v < 500$ mV/s for films of the dimension of that in Figure 1B). The peak width, ΔE_{fwhm}, of the wave for this electrode is 145 mV, considerably larger than the 90.6 mV expected for an ideal surface-attached couple with activity simply proportional to coverage.[59] The wave broadening is characteristic of polyelectrolyte coatings;[49,58-60] in the simplified Albery formulation[60] of the activity effect, which uses a modified Nernst equation, the Pt/poly-$[Ru(MeDSB)_3]^{2+/3+}$ film exhibits an "interaction parameter" term $g = 0.70$ (±0.02).

The other complexes of the type $[Ru(DSB)_x]^{2+}$ and $[Ru(MeDSB)_x]^{2+}$ in Table I exhibit similar electropolymerization characteristics and similar solution and surface Ru(III/II) formal potentials as shown in Table III. Qualitatively, the complexes containing greater numbers of DSB and MeDSB ligands undergo electropolymerization more rapidly (currents as illustrated in Figure 1A grow more rapidly), and DSB complexes generally electropolymerize more rapidly than their MeDSB analogues. These trends are summarized in the Γ^* values in Table III, which are measures of the relative rates of electropolymerization. A more quantitative assessment and comparison of the electropolymerization rates for the Ru and other complexes is given in a later section.

Table IV. Formal Potentials for the $[(L)_3Fe]^{2+}$, $[(L)_3Co]^{2+}$, and [(DSB)Re] Monomer Complexes and Their Electropolymerized Films

compd	$E^{\circ\prime}_{soln}$,[a] V vs. SSCE	$E^{\circ\prime}_{surf}$,[a] V vs. SSCE	Γ^*[b]
$[Fe(DSB)_3]^{2+/3+}$	0.90_5	0.93_5	1.8
$[Fe(MeDSB)_3]^{2+/3+}$	0.89	0.92_5	1.2
$[(DSB)Re(CO)_3Cl]^{0/+}$	−1.25		
$[Co(DSB)_3]^{2+/3+}$	0.18	0.20	0[c]
$[Co(DSB)_3]^{2+/+}$	−0.96	−0.97	
$[Co(MeDSB)_3]^{2+/3+}$	0.15	...	0[c]
$[Co(MeDSB)_3]^{2+/+}$	−0.99	...	

[a] In 0.1 M Et_4NClO_4/CH_3CN. [b] Relative rate of electropolymerization; $\Gamma^* = 1.0$ for $[(MeDSB)_3Ru]^{2+}$. [c] The integrity of the complex $[Co(L)_3]^{2+}$ is not maintained during electropolymerization; see text.

Os Complexes. The syntheses of monomeric Os polypyridine complexes containing vinyl-substituted ligands have proven difficult since the combination of the substitutionally inert Os and the necessarily forcing reaction conditions required cause thermal polymerization of the ligands. Generally, it has been necessary[36] to prepare first a complex that has a weakly bound solvent molecule before introduction of vpy or vbpy. The thermal stability of the DSB and MeDSB ligands simplifies the synthesis, enabling complexes of the type $[Os(L)_3]^{2+}$ and $[OsCl_2(L)_2]$ to be prepared in high yield with use of the solvents 2-(2-methoxyethoxy)ethanol and 2-methoxyethanol, respectively. Six complexes with variable numbers of DSB and bpy ligands ($[(DSB)_{3-n}Os(bpy)_n](PF_6)_2$) and of MeDSB and bpy ($[(MeDSB)_{3-n}Os(bpy)_n](PF_6)_2$) and the complex $[(DSB)_2Os(CO)Cl](PF_6)$, described below, were prepared. All of the complexes exhibited a reversible Os(II/III) cyclic voltammetric wave in CH_3CN and electropolymerization patterns analogous to those in Figure 1A, forming smooth electroactive films. The relative electropolymerization rates and a comparison of Os(III/II) formal potentials of the monomer complex solutions and of their polymeric films are given in Table III.

Fe Complexes. $[Fe(DSB)_3]^{2+}$ and $[Fe(MeDSB)_3]^{2+}$ exhibit electrochemistry similar to that of their Ru and Os analogues and can be reductively electropolymerized from CH_3CN solutions to form smooth, adherent films on Pt. As discussed in a later section, $[Fe(DSB)_3]^{2+}$ is, in fact, the most rapidly polymerizing compound ($\Gamma^* = 1.8$, Table III) presented here; 25 cyclical potential scans at 100 mV/s in a 0.67 mM solution resulted in ca. 100 monolayers of electroactive metal complex in the film. Films up to 5.4×10^{-8} mol/cm^2 that are fairly uniform have been prepared from this complex. The formal potentials of the monomer complexes and their polymer films are listed in Table IV.

Co Complexes. Since the $[Co(bpy)_3]^{2+/3+}$ electron self-exchange rate constant is known to be considerably smaller than those of its Fe, Ru, and Os analogs,[61,62] the preparation of intact poly-$[Co(DSB)_3]^{2+}$ or poly-$[Co(MeDSB)_3]^{2+}$ films would be useful from a comparative point of view. In 0.1 M Et_4NClO_4/CH_3CN, $[Co(DSB)_3]^{2+}$ exhibits quasi-reversible Co(III/II) and Co(II/I) couples at +0.18 and −0.96 V vs. SSCE, respectively, and a series of ill-defined waves at more reducing potentials. Successive scanning through the Co(III/II) and Co(II/I) couples results in little or no polymerization. The complex $[Co(MeDSB)_3]^{2+}$ behaves similarly. That extensive polymerization does not occur is disappointing but not especially surprising, given the metal-

(58) Brown, A. P.; Anson, F. C. *Anal. Chem.* **1977**, *49*, 1589.
(59) Smith, D. F.; Willman, K. W.; Kuo, K. N.; Murray, R. W. *J. Electroanal. Chem. Interfacial Electrochem.* **1979**, *95*, 217.
(60) Albery, W. J.; Boutelle, M. G.; Colby, P. J.; Hillman, A. R. *J. Electroanal. Chem. Interfacial Electrochem.* **1982**, *133*, 135.
(61) Przytas, T. J.; Sutin, N. *J. Am. Chem. Soc.* **1973**, *95*, 5545.
(62) Chan, M. S.; Wahl, A. C. *J. Phys. Chem.* **1978**, *82*, 2543.

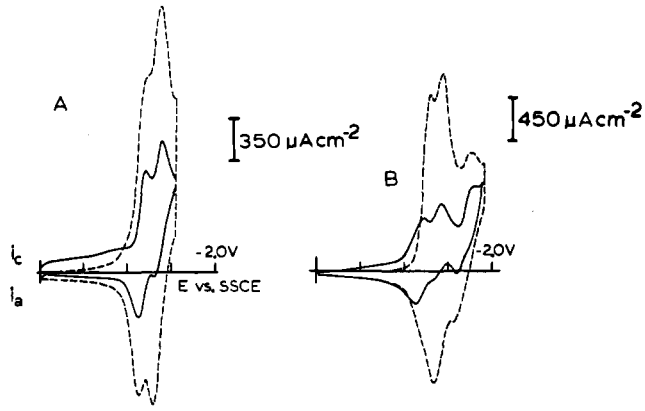

Figure 2. Cyclic voltammetry of 1.0 mM $[(DSB)_2Os(CO)Cl]^+$ solution in 0.1 M Et_4NClO_4/CH_3CN at 100 mV/s: (A) scans 1 (—) and 31 (---) from 0 to −1.55 V vs. SSCE; (B) scans 1 (—) and 28 (---) from 0 to −1.9 V vs. SSCE.

centered nature of the two couples. Extension of the potential scans to more negative potentials does result in electropolymerization, as evidenced by increases in the peak currents and the formation of a yellow film on the electrode. The cyclic voltammetric response of the coated electrode in fresh 0.1 M Et_4NClO_4/CH_3CN electrolyte shows a greatly diminished Co(III/II) wave and several other couples, but these slowly decay with continued potential scans. The formal potentials of the poly-$[Co(DSB)_x]^{3+/2+,2+/+}$ waves are given in Table IV. It is known that highly reduced forms of $[Co(bpy)_3]^{2+}$ undergo loss of bpy on the cyclic voltammetric time scale,[63] so that the DSB and MeDSB complexes have likely suffered a similar fate during electropolymerization.

$[(DSB)_2M(CO)Cl]^+$. In 0.1 M Et_4NClO_4/CH_3CN solutions, the complex $[(DSB)_2Os(CO)Cl]^+$ exhibits a reversible Os(II/III) cyclic voltammetric wave at 1.06 V vs. SSCE, two reversible DSB ligand reductions at −1.17 and −1.35 V, and an irreversible reduction wave at ca. −1.7 V. Repetitive potential scanning through the first two waves (0 to −1.55 V as in Figure 2A) results in a steady increase in the peak currents (dashed line in Figure 2A), indicating electropolymerization is occurring. When the cyclical potential scans are extended to −1.85 V (encompassing the third reduction), film growth is again evident (dashed line in Figure 2B), but now the first two waves begin to merge and increase more rapidly than the third wave. A polymer film is visibly evident on the electrode in both cases.

Cyclic voltammetry of the two polymer-coated electrodes prepared in Figure 2 is shown in Figure 3. The polymer film prepared by scanning through only the two DSB ligand waves (i.e., between 0 and −1.55 V) displays (Figure 3A) a well-defined Os(II/III) wave at 1.10 V (solid line in Figure 3A), which matches the formal potential of the monomer complex. The same film, at more positive potentials, also displays a smaller, irreversible, and unstable oxidation wave at 1.72 V (dashed line in Figure 3A). Including the more positive oxidation wave in the potential scan causes the main poly-$[(DSB)_2Os(CO)Cl]^{+/2+}$ wave at 1.10 V to decrease by ca. 6% upon the first cyclical potential scan, but it is stable thereafter. The irreversible, more positive oxidation wave at $E_{p,a}$ = 1.72 V likely represents a certain amount of poly-$[(DSB)_2Os(CO)(CH_3CN)]^{2+/3+}$ sites in the polymer film caused by substitution of CH_3CN for Cl^- during reductive electropolymerization. Substitution of CH_3CN for Cl^- in $[(bpy)_2OsCl_2]$ shifts $E^{o\prime}$ of the Os(II/III) couple positively by 450 mV;[56] no data are available for $[(bpy)_2Os(CO)(CH_3CN)]^{2+/3+}$. The wave at 1.72 V is small, showing that only a small amount of solvolysis occurs, probably in the doubly reduced $[(DSB)_2Os(CO)Cl]^-$ species. Extension of the electropolymerizing potential scan to −1.6 V yields a polymer film that now exhibits a poly-$[(DSB)_2Os(CO)(CH_3CN)]^{2+/3+}$ wave at 1.72 V, which, on the initial scan, is as large as the poly-$[(DSB)_2Os(CO)Cl]^{+/2+}$ wave at 1.10 V.

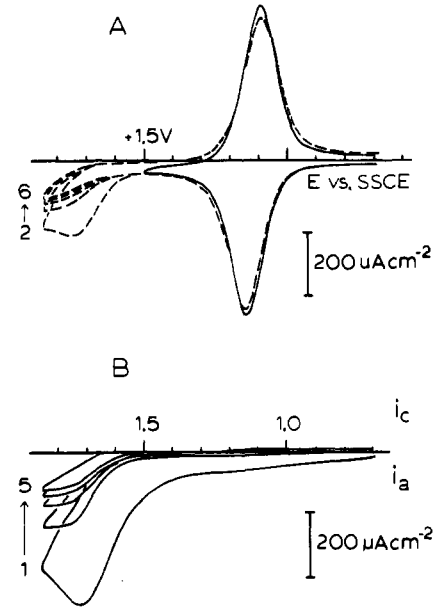

Figure 3. Cyclic voltammetry of electrodes from Figure 2 in 0.1 M Et_4NClO_4/CH_3CN at 100 mV/s: (A) electrodes from Figure 2A; (B) electrodes from Figure 2B.

Cyclic voltammetry of the polymer prepared in Figure 2B by scanning through all three reduction waves (i.e., between 0 and −1.85 V) is illustrated in Figure 3B. No poly-$[(DSB)_2Os(CO)Cl]^{+/2+}$ wave is evident now at all, only an irreversible, oxidation wave at 1.7 V, presumably again the poly-$[(DSB)_2Os(CO)(CH_3CN)]^{2+/3+}$ couple, which decays noticeably with continued potential scanning. Apparently, potential scanning through all three reduction waves leads to complete substitution of CH_3CN for Cl^- in the monomeric complexes that become incorporated into the polymer film.

The $[(DSB)_2Ru(CO)Cl]^+$ analogue of the above complex is interesting because it is a synthetic precursor to $[(DSB)_2Ru(CO)H]^+$, the bpy analogue of which is an established water-gas shift reagent.[64,65] This complex exhibits a reversible M(II/III) solution couple, at 1.24 V (Table III). Under the conditions employed thus far, however, the ligand-localized reduction waves are (chemically) irreversible. It appears that extensive substitution of CH_3CN for Cl^- occurs during the reduction process. The formal potential of the poly-$[(DSB)_2Ru(CO)(CH_3CN)]^{2+/3+}$ couple should be shifted positively by ~600 mV by the substitution (similar to the case for the osmium analogue) and thus would not be electrochemically accessible in our CH_3CN solvent window. X-ray photoelectron spectroscopy indicates that there is no Cl^- present in the polymer films, whereas XPS studies on powders of the monomeric complex show quantitatively the expected Cl band. In addition, there is no evidence of the poly-$[(DSB)_2Ru(CO)Cl]^{+/2+}$ couple in the electrochemistry of the films.

Re Complexes. The $[(DSB)Re(CO)_3Cl]$ complex is insoluble in acetonitrile, and so the electrochemical behavior was examined in solvent mixtures of CH_3CN/CH_2Cl_2. A reversible reduction wave, probably ligand based, appears at approximately −1.25 V (vs. SSCE) in a 9:1 CH_3CN/CH_2Cl_2 solvent mixture, followed by an irreversible reduction wave at −1.45 V. Overall, the electrochemistry is much more complex than that of the $[(bpy)Re(CO)_3Cl]$ analogue.[65]

Bipyridine analogues of $[(DSB)Re(CO)_3Cl]$ are known to catalytically reduce carbon dioxide.[66-68] One objective of syn-

(63) Margel, S.; Smith, W.; Anson, F. C. *J. Electrochem. Soc.* **1978**, *125*, 241.

(64) Choudhury, D.; Cole-Hamilton, D. J. *J. Chem. Soc., Dalton Trans.* **1982**, 1885.

(65) Tanaka, K.; Morimoto, M.; Tanaka, T. *Chem. Lett.* **1983**, 901.

(66) Sullivan, B. P.; Bolinger, C. M.; Conrad, D.; Vining, W. J.; Meyer, T. J. *J. Chem. Soc., Chem. Commun.* **1985**, 1414.

thesizing the $[(DSB)Re(CO)_3Cl]$ complex was to transfer the CO_2 catalysis to its polymer films on the electrode surface.[67] Unfortunately, electropolymerization could not be obtained in the CH_3CN/CH_2Cl_2 solvent. We have found that solutions of the $[(DSB)Re(CO)_3Cl]$ monomer, however, do catalyze the reduction of CO_2 in the CH_2Cl_2/CH_3CN solvent mixture, resulting in copious evolution of gas (CO and H_2 are known to be products of the reduction) from the electrode surface.

Polymerization Efficiency. As previously stated, complexes of the type $[M(DSB)_x]$ and $[M(MeDSB)_x]$ form electropolymerized films more slowly than do their vbpy and vpy analogues. The relative inertness of the olefinic bond in DSB and MeDSB that proved to be useful in the synthesis of the metal complex monomers also decreases the reactivity toward electropolymerization. For example, 15 cyclical potential scans through 2 vbpy ligand reduction waves in a 0.7 mM $[(vbpy)_3Ru]^{2+}$ solution results in a polymer film with an electroactive coverage of $\Gamma_T = 15 \times 10^{-9}$ mol/cm^2 as measured from the Ru(III/II) wave in fresh electrolyte,[69] while 25 cyclical potential scans through the 3 MeDSB reduction waves in a 0.67 mM $[(MeDSB)_3Ru]^{2+}$ solution (Figure 1A) results in a polymer film with $\Gamma_T = 6.3 \times 10^{-9}$ mol/cm^2, measured similarly. To compare the relative rates of electropolymerization for the DSB and MeDSB complex monomers presented here, we employed a previously described protocol.[36] In a solution of the monomer complex containing 2 mM concentration of the electropolymerizable *ligand* (i.e., 0.67 mM $M(L)_3$, 1.0 mM $M(L)_2$, or 2.0 mM M(L)) the potential was cyclically scanned 25 times at 100 mV/s over a 1-V window with a negative limit that is 100 mV more negative than $E^{\circ\prime}$ for the third ligand-localized wave (cf. Experimental Section). The film coverage Γ_T was measured from the metal(III/II) voltammogram in fresh 0.1 M Et_4NClO_4/CH_3CN electrolyte and was then divided by the similarly obtained Γ_T for the arbitrary standard compound $[Ru(MeDSB)_3]^{2+}$. This ratio is given as Γ^* in Tables III and IV. For the less efficiently polymerizing compounds (e.g., $[(MeDSB)_2Ru(CH_3CN)_2]^{2+}$) more than 25 cyclical potential scans were employed, and assuming Γ_T is proportional to the number of scans,[36] Γ^* was scaled accordingly.

Before discussing the implications of the Γ^* electropolymerization efficiencies, several elements of surface coating by electropolymerization should be noted. During potential scanning, reduced metal complex monomers may react either with each other, with coupling then terminated to give a net (hydro)*dimer*ization step, or with unreduced monomers as the beginning of a chain polymerization process. Our previous mechanistic study[36] on the electropolymerization of related monomers indicated that both routes are important. Oligomer/polymer complexes thus formed can diffuse away from the electrode, or if they are formed sufficiently rapidly and are sufficiently insoluble, they precipitate on the electrode surface. Coupling doubtless also occurs between monomers and polymer film already formed, but the element of precipitation is very important. It should be stressed that our Γ_T cyclic voltammetric assay of polymer formation detects only that portion of the coupling product that has precipitated on or otherwise coupled to the electrode. Any oligomer/polymer that diffuses away from the electrode surface before precipitating is *not* detected. The Γ^* value is thus a convolution of the coupling/polymerization rate and the solubility of the electrogenerated oligomer/polymers.

A comparison of the Γ^* values in Tables III and IV indicates several consistent trends. First, all of the DSB complexes of Ru have higher Γ^* values than their MeDSB analogues (Table III). The slightly higher solubility of the MeDSB vs. DSB metal complex monomers may be responsible for this small difference; the electrogenerated MeDSB oligomers near the electrode surface may be more soluble and precipitate less readily on the electrode. Second, in the $[(L)_{3-n}M(bpy)_n]^{2+}$ (n = 0–2) series, the Γ^* values logically correlate with the number of electropolymerizable ligands on the metal complex for both Os and Ru (Table III). This occurs even though the concentrations of monomers in the electropolymerization Γ^* measurement are normalized and has been observed previously.[36] We believe the main effect is that *successive* (hydro)dimerizations can occur for a complex bearing more than one DSB or MeDSB ligand, which increases oligomer chain length and thereby enhances precipitation. Finally, the Γ^* values for the complexes $[M(L)_3]$ fall in the order Os < Ru < Fe by comparisons between Tables III and IV. This trend is explicable in terms of the extent of metal–ligand orbital mixing for the series $[M(bpy)_3]^{2+}$, which, as inferred from spectroscopic studies,[70,71] is in the order Os > Ru > Fe. Consequently, the reduction of $[Fe(L)_3]^{2+}$ yields a "more ligand-localized" anion radical and thus a more reactive monomer. Solubility differences can also play a subtle role.

Table V. Electron Diffusion through poly-$[M(DSB)_x]^{2+/3+}$ Films

polymer film	$10^9\Gamma_T$, mol/cm^2	g	$D_e^{1/2}C_T$,[a] mol/(cm^2 s$^{1/2}$)
poly-$[Fe(DSB)_3]^{2+/3+}$	3.5–20	0.87	3.2 (±0.6) × 10^{-8}
poly-$[Ru(DSB)_3]^{2+/3+}$	3.3–12	0.79	1.19 (±0.24) × 10^{-7}
poly-$[Os(DSB)_3]^{2+/3+}$	6.5–12	0.71	8.9 (±1.3) × 10^{-8} [b]
poly-$[(DSB)_2Ru(bpy)]^{2+/3+}$	16–21	0.84	1.24 (±0.21) × 10^{-7}
poly-$[Ru(MeDSB)_3]^{2+/3+}$	11–14	0.70	1.34 (±0.7) × 10^{-7}

[a] Measured with $[Ru(bpy)_2Cl_2]$ as the solution substrate unless noted otherwise. [b] Measured with $[Os(bpy)_2Cl_2]$ as the solution substrate.

Electron Transport (Diffusion) in Redox Polymers. Electron transport through polymers bearing fixed, electronically localized redox sites is believed[41,52,72] to occur by electron self-exchange reactions between neighboring oxidized and reduced sites in the polymer films. Factors affecting the rate of the self-exchange reaction include the intrinsic barrier to self-exchange for the couple, polymer lattice restraints on the redox site, and mobilities of charge-compensating counterions within the polymer matrix. The available experimental quantity characterizing electron transport in the films is the electron diffusion coefficient, D_e, since the electrochemical process produces a charge flow that follows Fick's diffusion laws. D_e was measured for the polymers indicated in Table V by the mediation method of Ikeda,[49] which involves oxidation of a bulky, nonpermeating solute complex N(II) at the polymer–solution boundary of a polymer film on a rotating-disk electrode:

$$\text{Pt/poly-[M(III)]} + \text{N(II)} \rightarrow \text{Pt/poly-[M(II)]} + \text{N(III)} \quad (1)$$

The external metal couple chosen has a formal potential $E^{\circ\prime}_{SUB}$ that is quite negative (>500 mV) of the formal potential for the polymer, poly-[M(III/II)], couple in order to ensure that the cross-reaction in eq 1 is rapid. The resulting steady-state current on the rising portion of the voltammetric wave is controlled by the rate of electron diffusion between the electrode/polymer and polymer/solution interfaces and follows the relation

$$i = nFA(D_eC_T^2/\Gamma_T)\exp[(gnF/RT)(E - E^{\circ\prime}_{surf})] \quad (2)$$

where C_T is the concentration of M sites in the film and g is the Albery interaction/activity parameter.[60] At sufficiently positive potentials, the rate of electron diffusion becomes more rapid than the mass transport of the N(II) couple to the polymer/solution interface, and then a N(II)-mass-transport-limited plateau current prevails. The distinctive shape of this type of rotated-disk voltammogram, which rises gradually and abruptly plateaus, is shown in Figure 4A, where a Pt/poly-$[Fe(DSB)_3]^{2+}$ electrode serving

(67) Hawecker, J.; Lehn, J. M.; Ziessel, R. *J. Chem. Soc., Chem. Commun.* **1983**, 536; **1984**, 328; **1985**, 56.
(68) O'Toole, T. R.; Margerum, L. D.; Westmoreland, T. D.; Vining, W. J.; Murray, R. W.; Meyer, T. J. *J. Chem. Soc., Chem. Commun.* **1985**, 1416.
(69) Leidner, C. R. Ph.D. Dissertation, The University of North Carolina, 1984.
(70) Kober, E. M.; Meyer, T. J. *Inorg. Chem.* **1985**, *24*, 106.
(71) Kober, E. M.; Marshall, J. L.; Dressick, W. J.; Sullivan, B. P.; Casper, J. V.; Meyer, T. J. *Inorg. Chem.* **1985**, *24*, 2755.
(72) Kaufman, F. B.; Schroeder, A. H.; Engler, E. M.; Kramer, S. R.; Chambers, J. Q. *J. Am. Chem. Soc.* **1980**, *102*, 483.

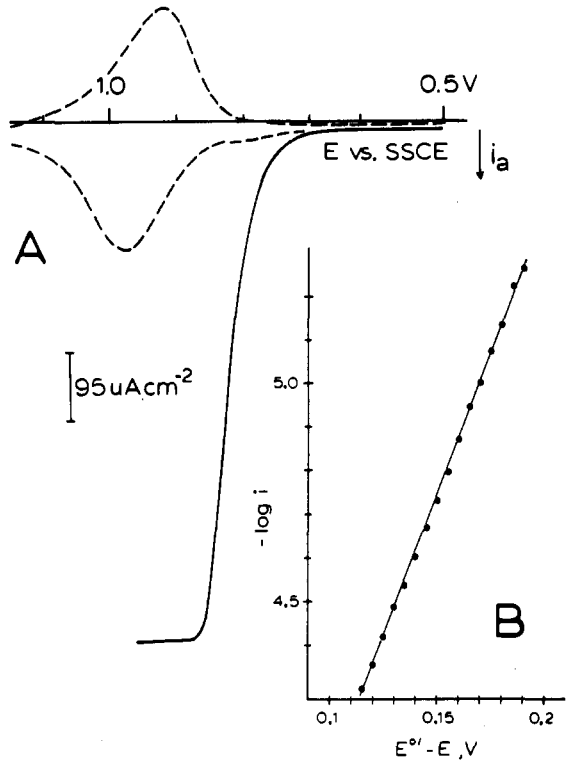

Figure 4. (A) Cyclic voltammetric (---) response of a Pt/poly-[Fe(DSB)$_3$]$^{2+}$ electrode with Γ_T = 7.7 × 10^{-9} mol/cm^2 and rotated-disk voltammogram (—) at the same electrode in 0.38 mM [(bpy)$_2$RuCl$_2$] solution, in 0.1 M Et_4NClO_4/CH_3CN (ω = 8100 rpm; v = 2 mV/s (—) and 100 mv/s (---). (B) Plot of -log i vs. $E°'_{surf} - E$ of eq 2, for voltammogram (—) in Figure 4A.

as the poly-[M(III/II)] couple with Γ_T = 7.7 × 10^{-9} mol/cm^2 oxidizes a 0.38 mM [(bpy)$_2$RuCl$_2$] solution (serving as N(II)). The rising portion of voltammetric waves as in Figure 4A is accurately described in eq 2 as shown in Figure 4B, and the abruptly attained i_{lim} plateau exhibits Levich behavior (i_{lim} is proportional to the square root of the rotation rate). The plot in Figure 4B yields g = 0.78 from the slope and $D_e^{1/2}C_T$ = 3.5 × 10^{-8} mol/(cm^2 s$^{1/2}$) from the intercept. The average g and $D_e^{1/2}C_T$ values for four different poly-[Fe(MeDSB)$_3$]$^{2+/3+}$ films are given in Table V as are similar results for Os and Ru polymers.

Several interesting points can be drawn from the electron diffusion data in Table V. First, for the three [M(DSB)$_3$]$^{2+}$-based (M = Fe, Ru, Os) polymers, the product $D_e^{1/2}C_T$ increases in the order Fe < Os < Ru. This is unexpectedly different from the order Fe < Ru < Os for [M(bpy)$_3$]$^{2+/3+}$ self-exchange in acetonitrile.[62] The origin of the difference is not clear, but it can be taken as a contribution to rate control from polymer chain mobility (rather than intrinsic barriers), as variations in the concentrations C_T of metal redox sites in the polymers, or as a combination of the two. Recall that the [Fe(DSB)$_3$]$^{2+}$ monomer electropolymerizes nearly 10× more rapidly than does [Os(DSB)$_3$]$^{2+}$. The differences in rate of polymer growth could be a source of a structural difference affecting chain mobility or relative site dispositions. Whatever the basis for the differences, it is worth noting that the Ru–DSB polymers have as high a value of $D_e^{1/2}C_T$ as any metalated polymer film measured in our laboratory. A second point is that Pt/poly-[Ru(DSB)$_3$]$^{2+}$ and Pt/poly-[(DSB)$_2$Ru(bpy)]$^{2+}$ films have experimentally equal electron diffusion rates. This implies that the redox sites in the two polymers undergo self-exchange reactions with equal facility, despite the opportunity for decreased site mobility (more cross-linking) in the former polymer film. While $D_e^{1/2}C_T$ for Pt/poly-[(DSB)Ru(bpy)$_2$]$^{2+}$ would have provided an interesting comparison in this regard, its measurement was precluded by its high permeability to the N(II) complex probe (vide infra). A third point is that Pt/poly-[Ru(DSB)$_3$]$^{2+}$ and Pt/poly-[Ru(MeDSB)$_3$]$^{2+}$ have essentially equal electron diffusion rates. Not surprisingly, $D_e^{1/2}C_T$ is insensitive to substitution of

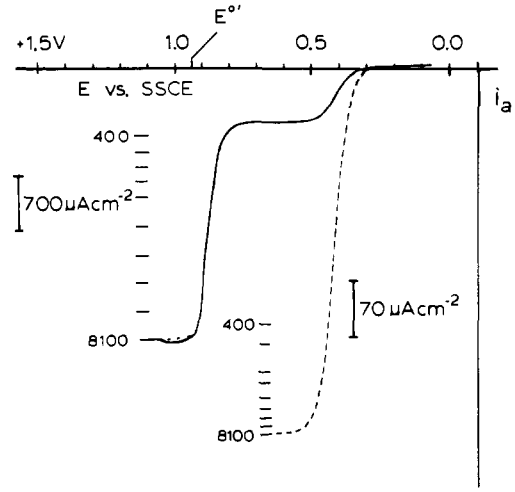

Figure 5. Rotated-disk voltammetry of Pt/poly-[Fe(DSB)$_3$]$^{2+}$ electrode with Γ_T = 17.8 × 10^{-9} mol/cm^2 in 0.31 mM ferrocene solution in 0.1 M Et_4NClO_4/CH_3CN at 1 mV/s and ω = 8100 rpm. For the left-hand voltammogram (—), limiting currents are shown for ω = 400, 625, 900, 1200, 1600, 2500, 3600, 4900, 6400, and 8100 rpm. For the expanded-scale voltammogram (---), limiting currents are shown for 400, 625, 900, 1200, 1600, 2500, 3600, 4900, 6400, and 8100 rpm.

methyl groups for hydrogens on the DSB ligand.

Permeability of Pt/poly-[(DSB)$_{3-n}$M(bpy)$_n$]$^{2+}$ Films. In the electron diffusion measurements above, the Pt/poly-[(DSB)$_{3-n}$M(bpy)$_n$]$^{2+}$ films are sufficiently thick, and the substrate complex N(II) in eq 1 sufficiently bulky, that currents due to permeation of N(II) through the polymer film to the Pt/polymer interface are negligibly small. If these conditions are changed, as we have shown previously,[50] permeation currents can be seen and serve to measure the properties of the polymer film as a membrane barrier coating the electrode. Figure 5 shows an example. Ferrocene is oxidized at a naked rotated Pt disk electrode in a wave (not shown) at 0.42 V vs. SSCE. When the rotated-disk electrode is coated with a Γ_T = 7.7 × 10^{-9} mol/cm^2 Pt/poly-[Fe(DSB)$_3$]$^{2+/3+}$ film, the previous wave at 0.42 V is greatly depressed, because the ferrocene must now diffuse through the polymer film to become oxidized at the Pt/polymer interface at the 0.45-V potential. At more positive potentials, the remainder of the ferrocene (that does not permeate) is oxidized in a mediation wave (solid line in Figure 5) analogous to that of Figure 4A. The ferrocene permeation wave in the solid-line voltammogram of Figure 5 is shown on an expanded scale (dashed line), where we also see the dependence of its limiting current i_{lim} on the electrode rotation rate ω. The permeating limiting currents i_{lim} do not follow Levich behavior (Figure 6A, solid line) and are considerably smaller than mass-transport-limited currents (dashed line in Figure 6A). The permeation currents follow the equation

$$\frac{1}{i_{lim}} = \frac{1}{0.62nFAD_s^{2/3}\nu^{-1/6}\omega^{1/2}C_s} + \frac{1}{nFAD_{s,pol}C_sC_T/\Gamma_T} \quad (3)$$

where the permeability is given as the product $PD_{s,pol}$, where P and $D_{s,pol}$ are the partition coefficient for ferrocene into and diffusion coefficient within the polymer film. The i_{lim} currents in Figure 6A when plotted according to eq 3 give a linear plot (Figure 6B), the intercept of which gives $PD_{s,pol}$ = 3.7 × 10^{-8} cm^2/s for ferrocene in this particular polymer. The average of several permeation experiments with ferrocene and Pt/poly-[Fe(DSB)$_3$]$^{2+}$ (Table VI) yields $PD_{s,pol}$ = 3.9 (±0.8) × 10^{-8} cm^2/s. Analogous permeation measurements with films of the same polymer and the larger complex [Ru(bpy)$_2$Cl$_2$] show that permeation occurs much more slowly, with $PD_{s,pol} \approx$ 1.2 (±0.2) × 10^{-9} cm^2/s (Table VI).

Permeation results for the six DSB polymer films shown in Table VI reveal several structure-related phenomena. For example, the extent of cross-linking in the Ru series of DSB polymers can be inferred from the variation of film permeability with the number of polymerizable ligands. Ferrocene permeates through

Table VI. Permeability of poly-$[M(DSB)_x]^{2+}$ Films

polymer film	external complex	$PD_{s,pol}C_T$, mol/(cm s)	$PD_{s,pol}$,[a] cm^2/s
poly-$[Fe(DSB)_3]^{2+}$	ferrocene	$5.8\ (\pm1.1) \times 10^{-11}$	$3.9\ (\pm0.8) \times 10^{-8}$
	$[Ru(bpy)_2Cl_2]$	$1.8\ (\pm0.3) \times 10^{-12}$	$1.2\ (\pm0.2) \times 10^{-9}$
poly-$[Ru(MeDSB)_3]^{2+}$	ferrocene	$6.2\ (\pm2.2) \times 10^{-11}$	$4\ 1\ (\pm1.5) \times 10^{-8}$
	$[Ru(bpy)_2Cl_2]$	$1.2_6\ (\pm0.34) \times 10^{-11}$	$8.4\ (\pm2.3) \times 10^{-8}$
poly-$[Ru(DSB)_3]^{2+}$	ferrocene	$6.7\ (\pm1.3) \times 10^{-11}$	$4.5\ (\pm1.1) \times 10^{-8}$
	$[Ru(bpy)_2Cl_2]$	$2.69\ (\pm0.7) \times 10^{-12}$	$1.8\ (\pm0.6) \times 10^{-9}$
poly-$[Os(DSB)_3]^{2+}$	$[Os(bpy)_2Cl_2]$	$4.2\ (\pm2.7) \times 10^{-12}$	$2.8\ (\pm1.8) \times 10^{-9}$
poly-$[(DSB)_2Ru(bpy)]^{2+}$	ferrocene	$7.0\ (\pm0.6) \times 10^{-11}$	$4.7\ (\pm0.4) \times 10^{-8}$
	$[Ru(bpy)_2Cl_2]$	$4.0\ (\pm1.5) \times 10^{-12}$	$2.7\ (\pm1.0) \times 10^{-9}$
poly-$[(DSB)Ru(bpy)_2]^{2+}$	ferrocene	$7.1\ (\pm0.7) \times 10^{-10}$	$4.7\ (\pm0.5) \times 10^{-7}$
	$[Ru(bpy)_2Cl_2]$	$1.1_8\ (\pm0.4) \times 10^{-10}$	$7.8\ (\pm0.25) \times 10^{-8}$

[a] Calculated by assuming $C_T = 1.5$ M for each film.

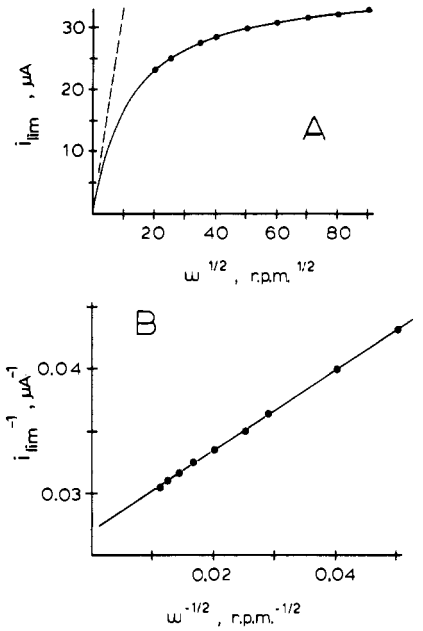

Figure 6. (A) Plot (—) of i_{lim} of the permeation wave (- - -) in Figure 5 vs. $\omega^{1/2}$. Limiting currents were measured at 0.65 V. The dashed line is the mass-transfer-limited current at a naked Pt electrode of the same area. (B) Plot of i_{lim}^{-1} vs. $\omega^{1/2}$ for the same data according to eq 4. The line is least-squares fit.

poly-$[Ru(DSB)_3]^{2+}$ and poly-$[(DSB)_2Ru(bpy)]^{2+}$ films at nearly equal rates, and likewise, $Ru(bpy)_2Cl_2$ permeates through these two films at similar rates, although more slowly than ferrocene. The permeability of poly-$[(DSB)Ru(bpy)_2]^{2+}$ to ferrocene is, in contrast, 10 times greater than that of the other films. This film is also more permeable to $[Ru(bpy)_2Cl_2]$ than are the other films, and poly-$[(DSB)Ru(bpy)_2]^{2+}$ films show less discrimination on the basis of size (ferrocene vs. $[Ru(bpy)_2Cl_2]$) than the other polymer films. These results suggest that poly-$[Ru(DSB)_3]^{2+}$ and poly-$[(DSB)_2Ru(bpy)]^{2+}$ are cross-linked to about the same extent, while poly-$[(DSB)Ru(bpy)_2]^{2+}$ films are markedly less cross-linked and have a more open structure. (That poly-$[(DSB)_3Ru]^{2+}$ and poly-$[(DSB)_2Ru(bpy)]^{2+}$ films are similarly cross-linked was also inferred from the D_e results above.) It is also apparent from Table VI that, in a series of poly-$[Ru(MeDSB)_3]^{2+}$ films, $PD_{s,pol}$ is virtually insensitive to the central metal ion. This result indicates, as expected, that the central metal has little influence on cross-linking in the polymer films. Finally, the poly-$[Ru(DSB)_3]^{2+}$ and poly-$[Ru(MeDSB)_3]^{2+}$ films have equal permeabilities to ferrocene but different permeabilities to $Ru(bpy)_2Cl_2$. The latter polymer apparently has a more open structure than the former, but consistent with a sieving effect, the difference can only be detected with the larger, more size discriminating $[Ru(bpy)_2Cl_2]$ complex. Thus, substitution of methyl groups for hydrogens on the DSB ligand has an observable, though subtle, effect on polymer structure, as evidenced by the film permeability results.

Acknowledgment. This work was supported by the National Science Foundation, Office of Naval Research, and the Army Research Office—Durham. C.R.L. acknowledges fellowship support from the North Carolina Board of Governors. Helpful discussions and experimental assistance from S. Sillman and Drs. J. M. Calvert and W. R. Murphy are gratefuly acknowledged.

Registry No. MeDSB, 106734-89-8; DSB, 1762-40-9; $[(DSB)_3Ru](PF_6)_2$, 106734-90-1; $[(DSB)_2Ru(bpy)](PF_6)_2$, 106761-09-5; $[(DSB)Ru(bpy)_2](PF_6)_2$, 106734-92-3; $[(MeDSB)_3Ru](PF_6)_2$, 106734-94-5; $[(MeDSB)_2Ru(bpy)](PF_6)_2$, 106734-96-7; $[(MeDSB)Ru(bpy)_2](PF_6)_2$, 106734-98-9; $(DSB)_2RuCl_2$, 106734-99-0; $(MeDSB)_2RuCl_2$, 106761-52-8; $[(DSB)_2Ru(CH_3CN)_2](PF_6)_2$, 106735-01-7; $[(MeDSB)_2Ru(CH_3CN)_2](PF_6)_2$, 106735-03-9; $[(DSB)_2Ru(pyrc)](PF_6)$, 106735-05-1; $[(DSB)_2Ru(bpym)](PF_6)_2$, 106761-54-0; $[(DSB)_2Ru(CO)Cl](PF_6)$, 106735-07-3; $[Fe(DSB)_3](PF_6)_2$, 106761-56-2; $[Fe(MeDSB)_3](PF_6)_2$, 106735-09-5; $[(DSB)_3Os](PF_6)_2$, 106735-11-9; $[(DSB)_2Os(bpy)](PF_6)_2$, 106735-13-1; $[(DSB)Os(bpy)_2](PF_6)_2$, 106735-15-3; $[(MeDSB)_3Os](PF_6)_2$, 106735-17-5; $[(MeDSB)_2Os(bpy)](PF_6)_2$, 106735-19-7; $[(MeDSB)Os(bpy)_2](PF_6)_2$, 106735-21-1; $(DSB)_2OsCl_2$, 106735-22-2; $(MeDSB)_2OsCl_2$, 106735-23-3; $[(DSB)_2Os(CO)Cl](PF_6)$, 106735-25-5; $[Co(DSB)_3](PF_6)_2$, 106779-97-9; $[Co(MeDSB)_3](PF_6)_2$, 106735-27-7; $(DSB)Re(CO)_3Cl$, 106735-28-8; $[Ru(DSB)_3]^{3+}$, 106735-29-9; $[(DSB)_2Ru(bpy)]^{3+}$, 106735-30-2; $[(DSB)Ru(bpy)_2]^{3+}$, 106735-31-3; $[Ru(MeDSB)_3]^{3+}$, 106735-32-4; $(MeDSB)_2Ru(bpy)]^{3+}$, 106735-33-5; $[(MeDSB)Ru(bpy)_2]^{3+}$, 106735-34-6; $[(DSB)_2Ru(CH_3CN)_2]^{3+}$, 106735-35-7; $[(MeDSB)_2Ru(CH_3CN)_2]^{3+}$, 106735-36-8; $[(DSB)_2Ru(pyrc)]^{2+}$, 106735-37-9; $[(DSB)_2Ru(bpym)]^{3+}$, 106735-38-0; $[(DSB)_2Ru(CO)Cl]^{2+}$, 106735-39-1; $[Os(DSB)_3]^{3+}$, 106735-40-4; $[(DSB)_2Os(bpy)]^{3+}$, 106735-41-5; $[(DSB)Os(bpy)_2]^{3+}$, 106735-42-6; $[Os(MeDSB)_3]^{3+}$, 106735-43-7; $[(MeDSB)_2Os(bpy)]^{3+}$, 106735-44-8; $[(MeDSB)Os(bpy)_2]^{3+}$, 106735-45-9; $[(DSB)_2Os(CO)Cl]^{2+}$, 106735-46-0; $[(DSB)_2OsCl_2]^{+}$, 106735-47-1; $[(DSB)_2OsCl_2]^{2+}$, 106735-48-2; $[(MeDSB)_2OsCl_2]^{+}$, 106735-49-3; $[(MeDSB)_2OsCl_2]^{2+}$, 106735-50-6; poly-$[Ru(DSB)_3](PF_6)_2$, 106761-57-3; poly-$[Ru(DSB)_3](PF_6)_3$, 106761-58-4; poly-$[(DSB)_2Ru(bpy)](PF_6)_2$, 106761-59-5; poly-$[(DSB)_2Ru(bpy)](PF_6)_3$, 106761-60-8; poly-$[(DSB)Ru(bpy)_2](PF_6)_2$, 106761-61-9; poly-$[(DSB)Ru(bpy)_2](PF_6)_3$, 106761-62-0; poly-$[Ru(MeDSB)_3](PF_6)_2$, 106761-63-1; poly-$[Ru(MeDSB)_3](PF_6)_3$, 106761-64-2; poly-$[(MeDSB)_2Ru(bpy)](PF_6)_2$, 106761-65-3; poly-$[(MeDSB)_2Ru(bpy)](PF_6)_3$, 106761-66-4; poly-$[(MeDSB)Ru(bpy)_2](PF_6)_2$, 106761-67-5; poly-$[(MeDSB)Ru(bpy)_2](PF_6)_3$, 106761-68-6; poly-$[(DSB)_2Ru(CH_3CN)_2](PF_6)_2$, 106761-69-7; poly-$[(DSB)_2Ru(CH_3CN)_2](PF_6)_3$, 106761-70-0; poly-$[(MeDSB)_2Ru(CH_3CN)_2](PF_6)_2$, 106761-71-1; poly-$[(MeDSB)_2Ru(CH_3CN)_2](PF_6)_3$, 106761-72-2; poly-$[(DSB)_2Ru(pyrc)](PF_6)$, 106761-73-3; poly-$[(DSB)_2Ru(pyrc)](PF_6)_2$, 106761-74-4; poly-$[(DSB)_2Ru(bpym)](PF_6)_2$, 106761-75-5; poly-$[(DSB)_2Ru(bpym)](PF_6)_3$, 106761-76-6; poly-$[Os(DSB)_3](PF_6)_2$, 106761-77-7; poly-$[Os(DSB)_3](PF_6)_3$, 106761-78-8; poly-$[(DSB)_2Os(bpy)](PF_6)_2$, 106761-79-9; poly-$[(DSB)_2Os(bpy)](PF_6)_3$, 106761-80-2; poly-$[(DSB)Os(bpy)_2](PF_6)_2$, 106761-81-3; poly-$[(DSB)Os(bpy)_2](PF_6)_3$, 106761-82-4; poly-$[Os(MeDSB)_3](PF_6)_2$, 106761-83-5; poly-$[(Os(MeDSB)_3](PF_6)_3$, 106761-84-6; poly-$[(MeDSB)_2Os(bpy)](PF_6)_2$, 106761-85-7; poly-$[(MeDSB)_2Os(bpy)](PF_6)_3$, 106761-86-8; poly-$[(MeDSB)Os(bpy)_2](PF_6)_2$, 106761-87-9; poly-$[(MeDSB)Os(bpy)_2](PF_6)_3$, 106761-88-0; poly-$[(DSB)_2Os(CO)Cl](PF_6)$, 106761-89-1; poly-$[(DSB)_2Os(CO)Cl](PF_6)_2$, 106761-90-4; $[Fe(DSB)_3]^{3+}$, 106735-51-7; $[Fe(MeDSB)_3]^{3+}$, 106735-52-8; $[(DSB)Re(CO)_3Cl]^{+}$, 106735-53-

9; $[Co(DSB)_3]^{3+}$, 106735-54-0; $[Co(DSB)_3]^{+}$, 106735-55-1; $[Co(MeDSB)_3]^{3+}$, 106735-56-2; $[Co(MeDSB)_3]^{+}$, 106735-57-3; poly-$[Fe(DSB)_3](PF_6)_2$, 106761-91-5; poly-$[Fe(DSB)_3](PF_6)_3$, 106761-92-6; poly-$[Fe(MeDSB)_3](PF_6)_2$, 106761-93-7; poly-$[Fe(MeDSB)_3](PF_6)_3$, 106761-94-8; poly-$[Co(DSB)_3](PF_6)_2$, 106761-96-0; poly-$[Co(DSB)_3](PF_6)_3$, 106761-97-1; poly-$[Co(DSB)_3](PF_6)$, 106761-98-2; $Re(CO)_5Cl$, 14099-01-5; $(bpy)_2RuCl_2$, 15746-57-3; $(NH_4)_2OsCl_6$, 12125-08-5; $Os(bpy)_2Cl_2$, 15702-72-4; Pt, 7440-06-4; 4,4′-dimethyl-2,2′-bipyridine, 1134-35-6; 4-methylbenzaldehyde, 104-87-0; benzaldehyde, 100-52-7; iodine, 7553-56-2; formic acid, 64-18-6; carbon dioxide, 124-38-9.

Contribution from the Department of Chemistry,
York University, North York, Ontario, Canada M3J 1P3

Synthesis, Aggregation, Electrocatalytic Activity, and Redox Properties of a Tetranuclear Cobalt Phthalocyanine

W. A. Nevin, W. Liu,[1a] S. Greenberg, M. R. Hempstead, S. M. Marcuccio, M. Melník,[1b]
C. C. Leznoff,* and A. B. P. Lever*

Received August 22, 1986

Using pentaerythritol as a framework, it has been possible to synthesize a tetranuclear phthalocyanine with a spiro type linkage. Electrochemical and spectroelectrochemical data are presented for the cobalt complex in the $Co^{III}Pc(-2)$, $Co^{II}Pc(-2)$, $Co^{I}Pc(-2)$, $Co^{III}Pc(-1)$, $Co^{II}Pc(-1)$, and $Co^{I}Pc(-3)$ oxidation levels. The Co(II) species aggregates very strongly, dimerizing with an aggregation constant in *o*-dichlorobenzene of 2.4×10^5 M^{-1}, 2 orders of magnitude greater than for the parent $Co^{II}TNPc$. Monolayers of the cobalt(II) species laid upon an ordinary pyrolytic graphite electrode are shown to electrocatalytically reduce oxygen more efficiently than previously described analogous mononuclear and binuclear phthalocyanines. The Co(II) tetranuclear species disproportionates into a 1:1 mixture of Co(I) and Co(III) species upon reaction with hydroxide ion in a nondonating or weakly donating solvent. A film containing $[Co^{I}TrNPc(-2)]_4^{4-}$ reduces nitrite ion in NaOH slowly, with oxidation to the Co(II) tetranuclear species.

Metal phthalocyanines (generally containing either cobalt or iron) have been implicated as electrocatalysts for the reduction of oxygen at a fuel cell cathode.[2-6] Ill-defined "dimeric" and polymeric phthalocyanines[6,7] are revealed to be more effective oxygen reduction electrocatalysts than their mononuclear congeners perhaps because the electrocatalyst can participate in a concerted fashion with the multielectron reduction (two electrons to hydrogen peroxide or four to water). This prompted us to design a series of polynuclear phthalocyanines, with the expectation that a multielectron redox catalyst might be designed, having enhanced properties relative to those of the common one-electron electrocatalysts.

The preparations of trinuclear[8] and binuclear phthalocyanines covalently linked by one-,[8] two-,[9] four-[9] and five-atom[10,11] bridges have recently been described. These phthalocyanines are linked at one benzene ring, the remaining benzene rings being substituted with neopentoxy groups to confer solubility in organic solvents. A preliminary discussion of the oxygen reduction capability of cobalt derivatives of these species has been reported.[12]

In general, we noted that these binuclear cobalt species were indeed more effective oxygen reduction catalysts to hydrogen peroxide (as indicated by kinetic current evaluation, of monolayers on ordinary pyrolytic graphite, immersed in 0.1 M NaOH) than their mononuclear analogues, though the improvement was not dramatic.

To be effective, it was necessary to reduce these electrocatalysts to form binuclear Co(I) species. Mechanistically, oxygen activation is believed to occur through formation of binuclear Co(III) peroxy species, but the degree of coupling between the halves of the binuclear species appears minimal, though not negligible, in the binuclear complexes.

We wished to prepare multinuclear phthalocyanines in which the phthalocyanine groups would be constrained to be cofacial. The previously prepared binuclear and trinuclear compounds could partially attain a cofacial conformation but were free to rotate so that a dynamic equilibrium existed between intramolecularly aggregated phthalocyanines in cofacial and isolated conformations. We believed that a tetranuclear phthalocyanine based on a pentaerythritol nucleus (Figure 1) could provide a multinuclear phthalocyanine in which two coupled pairs of phthalocyanine moieties would be so constrained by the geometry of the system, effectively a spiro arrangement, that the tetranuclear phthalocyanine would always consist of two pairs of phthalocyanines in a cofacial conformation.

This then suggested that a tetranuclear cobalt(II) phthalocyanine might be reduced to Co(I) with the possibility of four Co(I) atoms then being oxidized in a concerted fashion to Co(II) (four electrons) or Co(III) (eight electrons). Indeed the cobalt

(1) (a) Current address: Department of Chemistry, Yangzhou Teachers' College, Yangzhou, Jiangsu, People's Republic of China. (b) Department of Chemistry, Slovak Technical Institute, Bratislava, Czechoslovakia.
(2) Beck, F.; Dammert, W.; Heiss, J.; Hiller, H.; Polster, R. *Z. Naturforsch., A: Phys., Phys. Chem., Kosmophys.* **1973**, *28A*, 1009. Hirai, T.; Yamaki, J.; Yamaji, A. *J. Appl. Electrochem.* **1985**, *15*, 77. Van den Brink, F.; Visscher, W.; Barendrecht, E. *J. Electroanal. Chem. Interfacial Electrochem.* **1984**, *175*, 279; **1984**, *172*, 301; **1983**, *157*, 283, 305.
(3) Melendres, C. A.; Feng, X. *J. Electrochem. Soc.* **1983**, *130*, 811.
(4) Zecevic, S.; Simic-Glavaski, B.; Yeager, E.; Lever, A. B. P.; Minor, P. C. *J. Electroanal. Chem. Interfacial Electrochem.* **1985**, *196*, 339.
(5) Hirai, T.; Yamaki, J. *J. Electrochem. Soc.* **1985**, *132*, 2125.
(6) Appleby, A. J.; Fleisch, J.; Savy, M. *J. Catal.* **1976**, *44*, 281.
(7) Maroie, S.; Savy, M.; Verbist, J. J. *Inorg. Chem.* **1979**, *18*, 2560.
(8) Greenberg, S.; Marcuccio, S. M.; Leznoff, C. C.; Tomer, K. B. *Synthesis* **1986**, 406.
(9) Marcuccio, S. M.; Svirskaya, P. I.; Greenberg, S.; Lever, A. B. P.; Leznoff, C. C.; Tomer, K. B. *Can. J. Chem.* **1985**, *63*, 3057.
(10) Leznoff, C. C.; Greenberg, S.; Marcuccio, S. M.; Minor, P. C.; Seymour, P.; Lever, A. B. P.; Tomer, K. B. *Inorg. Chim. Acta* **1984**, *89*, L35.
(11) Leznoff, C. C.; Marcuccio, S. M.; Greenberg, S.; Lever, A. B. P.; Tomer, K. B. *Can. J. Chem.* **1985**, *63*, 623.
(12) Hempstead, M. R.; Leznoff, C. C.; Lever, A. B. P., to be submitted for publication.

0020-1669/87/1326-0891$01.50/0